

Short Communication

Lignocellulosic-derived catalysts for the selective oxidation of propane

M. Olga Guerrero-Pérez^{a,*}, Juana M. Rosas^a, Ricardo López-Medina^b, Miguel A. Bañares^b, José Rodríguez-Mirasol^a, Tomás Cordero^a

^a Departamento de Ingeniería Química, Universidad de Málaga, E-29071-Málaga, Spain

^b Catalytic Spectroscopy Laboratory, Instituto de Catálisis y Petroleoquímica (CSIC), Marie Curie, 2, E-28049-Madrid, Spain

ARTICLE INFO

Article history:

Received 29 November 2010

Received in revised form 3 March 2011

Accepted 7 March 2011

Available online 15 March 2011

Keywords:

VPO

Acrylic acid

Carbon support

Propane

Biomass

ABSTRACT

The formation of dispersed VPO phases on a lignocellulosic-based activated carbon results in a catalyst that is selective for the partial oxidation of propane, and stable under oxidizing conditions. The use of a stable activated carbon as a catalytic support for active VOx species during the partial oxidation of propane is described for the first time.

© 2011 Elsevier B.V. All rights reserved.

1. Introduction

The direct synthesis of acrylic acid from propane is an attractive process due to its use as raw material to make synthetic resins, paints, fibers, etc. Several million tons per year of acrylic acid is currently produced from propylene by a two-step gas phase oxidation process. Thus, the replacement of propylene with a lower-cost and more abundant feedstock such as propane is an important strategic alternative. Three groups of catalysts exhibit promising results for this process [1]: i) vanadium phosphate type; ii) heteropoly acids and salts and iii) multi-compound mixed metal oxides [2–4]. Despite all efforts, the low selectivity at high conversion limits its commercial viability [5], remaining selectivity as a key challenge.

The VPO catalytic system is attractive for alkane selective oxidation and it is successfully used in the industrial oxidation of n-butane to maleic anhydride. Supported VPO catalysts have many advantages since the support improves the mechanical strength, poison resistance, and heat transfer [6]. The nature of the specific support has a significant influence on the catalyst performance. In this sense, carbon materials are attractive as catalyst support since they can satisfy most of the desirable properties required for a suitable support: high surface area, chemical stability in both highly acidic and based media and, in addition, the chemistry of the carbon surface can be modulated [7]. However, carbon supports have not been used for oxidation reaction since they would gasify to CO₂ (or CO) in the presence of oxygen at relatively low temperatures. Nevertheless, it

has been shown [8] that it is possible to prepare carbon materials with a relatively large amount of phosphorus on the carbon surface by chemical activation of lignocellulosic materials with phosphoric acid. This activation procedure lead to phosphorus surface complexes in the form of COPO₃, CPO₃ and C₃P groups, which remain very stable on the carbon surface at relatively high temperatures and confer to the carbons a high oxidation resistance, acting as a physical barrier and blocking the active carbon sites for the oxidation reaction [8–11]. Following this idea, carbon nanotubes doped with phosphorus have been used as catalysts for the oxidative dehydrogenation of propane into propylene [12], but the use of activated carbons is more attractive, due to their low cost. Since different raw materials including biomass residues can be used for the preparation of activated carbons [13], this derives to a revalorization of the waste in a high valuable product, such as an activated carbon useful for catalytic applications. In the present study, several carbon-supported vanadium catalysts have been obtained by impregnation with vanadium solution on an oxidation-resistant activated carbon.

2. Experimental

Orange skin waste from Guadalhorce Valley (Málaga, Spain) was used as starting material for obtaining citrus skin-derived activated carbons. The raw material was washed with water, air-dried at room temperature for about one month and grinded and sieved to a particle size between 100 and 200 μm. The activation with phosphoric acid procedure has been reported before [8,11], the orange skin was impregnated with concentrated commercial H₃PO₄ (85 wt.%, Sigma Aldrich) at room temperature for 2 h, and dried for 24 h at 60 °C, with

* Corresponding author.

E-mail address: oguerrero@uma.es (M.O. Guerrero-Pérez).

an impregnation H_3PO_4 to orange skin weight ratio of 3. The impregnated citrus skin was thermally treated, at $500\text{ }^\circ\text{C}$, under continuous N_2 (purity 99.999%, Air Liquide) flow ($150\text{ cm}^3\text{ STP/min}$) in a conventional tubular furnace. The activation temperature was reached at a heating rate of $10\text{ }^\circ\text{C/min}$ and maintained for 2 h. The activated sample was cooled inside the furnace under the same N_2 flow and then washed with distilled water at $60\text{ }^\circ\text{C}$ until neutral pH and negative phosphate analysis in the eluate. The resulting activated carbon was denoted by ACP. This activated carbon was impregnated with a solution of NH_4VO_3 (purity 99.99%, Sigma Aldrich). The concentration of this solution contained the desired amount of vanadium ions depending on the sample formulation, since two samples were prepared with different vanadium coverages, 0.5 V/ACP and 1 V/ACP, where 0.5 and 1 indicates the number of vanadium atoms per nm^2 of carbon support, respectively. This solution was prepared by mixing ammonium metavanadate with a 0.5 M solution of oxalic acid (purity 99%, Sigma Aldrich), and was heated and stirred until clear before impregnating the support. The water excess was removed in a rotary evaporator at $80\text{ }^\circ\text{C}$ and at a reduced pressure of 10–40 mm Hg. The resulting solid was dried at $120\text{ }^\circ\text{C}$ for 24 h and then calcined at $250\text{ }^\circ\text{C}$ for 2 h in air.

The porous structure of the activated carbons was characterized by N_2 adsorption–desorption at $-196\text{ }^\circ\text{C}$ and by CO_2 adsorption at $0\text{ }^\circ\text{C}$, performed with a ASAP 2020 equipment (Micromeritics). From the N_2 isotherm, the apparent surface area ($A_{\text{BET}}^{\text{N}_2}$) was determined by applying the BET equation. The micropore volume ($V_{\text{DR}}^{\text{N}_2}$) was obtained by using the Dubinin–Radushkevich equation and the narrow mesopore volume was determined as the difference between the adsorbed volume of N_2 at a relative pressure of 0.95 and the micropore volume ($V_{\text{DR}}^{\text{N}_2}$). From the CO_2 adsorption data, the narrow micropore volume ($V_{\text{DR}}^{\text{CO}_2}$) was calculated using the Dubinin–Radushkevich equation. The pH of the sample suspension was determined as described by Bandosz et al. [14]. A sample of 0.4 g of dry carbon powder was added to 20 ml of water and the suspension was stirred overnight to reach equilibrium. Then the sample was filtered and the pH of solution was measured with a pH-meter. The surface acidity was studied by adsorption of pyridine (Py) carried out in a thermogravimetric system (CI Electronics) at $100\text{ }^\circ\text{C}$. The inlet partial pressure of the organic bases was 0.02 atm, and it was established saturating He with the corresponding organic base in a saturator at controlled temperature. After saturation of the sample, desorption is carried out at the adsorption temperature in Helium flow.

The surface chemistry of the samples was analyzed by X-ray photoelectron spectroscopy (XPS), performed with a 5700 C model Physical Electronics equipment, with Mg K α radiation (1253.6 eV). For a detailed study of the XPS peaks, the maximum of the C1s peak was reallocated at 284.5 eV and used as a reference to shift the other peaks. The deconvolution of the peaks was done using Gaussian–Lorentzian curves and a Shirley type background line. The XPS atomic ratios were obtained using the Phi Multipack software (Physical Electronics, Inc). Oxidation resistance of the different catalysts and the carbon support were obtained by non-isothermal thermogravimetric analyses, carried out in a CI electronics thermogravimetric system. The thermobalance automatically measures the weight of the sample and the temperature as a function of time. Experiments were carried out in air atmosphere, for a total flow rate of $150\text{ cm}^3\text{ (STP)/min}$, employing sample mass of approximately 10 mg. The sample temperature was increased from room temperature up to $900\text{ }^\circ\text{C}$ at a heating rate of $10\text{ }^\circ\text{C/min}$. Raman spectra were run with a single monochromator Renishaw System 1000 equipped with a cooled CCD detector ($-73\text{ }^\circ\text{C}$) and an Edge filter. The samples were excited with the 514 nm Ar^+ line; the spectral resolution was ca. 3 cm^{-1} and spectra acquisition consisted of 10 accumulations of 30 s. The spectra were obtained under dehydrated conditions (ca. 390 K, synthetic air) in a hot stage (Linkam TS-1500).

Activity measurements were performed using a conventional fixed-bed reactor. The design of the reactor has been made to minimize the void volume, since it has capillars up and downstream. The feed stream and effluents of the reactor were analyzed by an on-line gas-chromatograph equipped with flame ionization and thermal-conductivity detectors. The accuracy of the analytical determinations was checked for each test by verification that the carbon balance (based on the propane converted) was within the cumulative mean error of the determinations ($\pm 10\%$). The catalytic tests were made using 0.2 g of powder sample with particle dimensions in the 0.25–0.125 mm range. The axial temperature profile was monitored by a thermocouple sliding inside a quartz tube inserted into the catalytic bed. Tests were made using the following reaction feed composition (% volume): 20.4% O_2 , 12.5% propane and 15.9% steam in helium. The total flow rate was 40 ml/min, corresponding to 4800 h^{-1} gas hourly-space velocity (GHSV). The particle size of catalyst and the total flow were selected in order to avoid internal and external diffusion limitations. Product yields and selectivities were determined on the basis of the moles of propane feed and products, considering the number of carbon atoms in each molecule.

3. Results and discussion

Table 1 illustrates characterization data of the carbon-supported vanadium catalysts. As expected, both BET and external surface area values decrease with vanadium coverage, but total area remains high for the VPO supported catalysts. The relative atomic surface concentrations obtained by peak quantitative analysis are summarized in Table 2. The $\text{V}2p_{3/2}$ binding energies for the vanadium catalysts are 516.5 and 516.7 eV for 0.5 V/ACP and 1 V/ACP, respectively; characteristic of a mixture of V^{5+} and V^{4+} species. These BE values are lower than those reported for oxide-supported VPO catalysts on other supports, such as MCM-41, SiO_2 or SBA15 [6]. This suggests that the amount of reduced vanadium species is higher on the carbon-based support than on oxide supports. Carbon support must stabilize partially reduced vanadium sites, which are reported active for partial oxidation reactions [15,16] since partially reduced vanadium species (e.g. V^{4+}) are involved in the O-insertion to form acrylic acid on M2 phase, responsible for acrylic acid formation in the multicomponent Mo–V–Nb–Te–O catalytic system [17,18]; Also in the case of the VPO catalytic system, the active phase has been found to be $(\text{VO})_2\text{P}_2\text{O}_7$, with vanadium species as V^{4+} [19].

Since the pH of a carbon sample suspension provides information about the acidity and basicity of the surface, these values have been calculated according to the procedure described by Bandosz et al. [14]. As expected, the pH value for the activated carbon is quite low (3.31), indicative of a high amount of acid (surface phosphate groups retained on the carbon) sites on the surface [10,20]. The pH increases as vanadium coverage is increased, with values of 4.09 for 0.5 V/ACP and of 5.32 for 1 V/ACP, indicative that vanadium oxide dispersed species are titrating these phosphorus acid sites. In addition, pyridine adsorption experiments were performed with both catalysts and the results are shown in Fig. 1. It is well known that pyridine interacts with acidic sites because it has a lone electron pair at the nitrogen atom available for donation to a Lewis acidic site and because it can accept a proton from Brønsted sites. It can be observed in Fig. 1 that pyridine adsorption capacity for the sample with lower vanadium

Table 1
Structural parameters of P-modified carbon support (ACP) and V-supported catalysts (0.5 V/ACP and 1 V/ACP).

	$A_{\text{BET}}^{\text{N}_2}$ (m^2/g)	$V_{\text{DR}}^{\text{N}_2}$ (m^3/g)	$V_{\text{mes}}^{\text{N}_2}$ (cm^3/g)	$V_{\text{DR}}^{\text{CO}_2}$ (m^2/g)
ACP	1056	0.356	0.987	0.167
0.5 V/ACP	732	0.252	0.645	0.130
1 V/ACP	696	0.237	0.575	0.122

Table 2
XPS surface relative atomic concentrations.

	C1s	N1s	O1s	P2p	V2p	P/V
ACP	88.53	0.82	9.16	1.50	–	–
0.5 V/ACP	80.81	1.36	16.07	1.27	0.49	2.59
1 V/ACP	84.93	1.92	11.31	1.09	0.75	1.45

content (0.5 V/ACP) is approximately twice the capacity for 1 V/ACP, indicative of the higher amount of acid sites on the surface of the carbon support that is not covered by the VO_x species due to the higher free phosphate species content and low vanadium coverage (Table 2).

Fig. 2 illustrates thermogravimetric analysis profiles in air. These results indicate that the carbon support is resistant in air up to 500 °C, lowering this temperature to 400 °C when the activated carbon is impregnated with the vanadium species, enabling their use for propane oxidation reaction at ca. 375 °C without a significant gasification of the carbon support. In addition, catalysts were tested during 48 h under reaction conditions (Fig. 3) and the results clearly indicate that the catalysts are stable. Also the carbon balance during the oxidation experiments is consistent with the catalyst stability under reaction conditions. The carbon material presents negligible propane conversion, indicating that it is not able to activate the propane molecule at the reaction temperature. In the case of 0.5 V/ACP catalysts, with P/V = 2.59 (Table 2), the excess of phosphorous species leads to the formation of phosphorus acid sites on the surface of the sample, as was demonstrated with the pyridine adsorption experiments (Fig. 1). The vanadium species present in 0.5 V/ACP sample are able to activate the propane molecule, and then, these

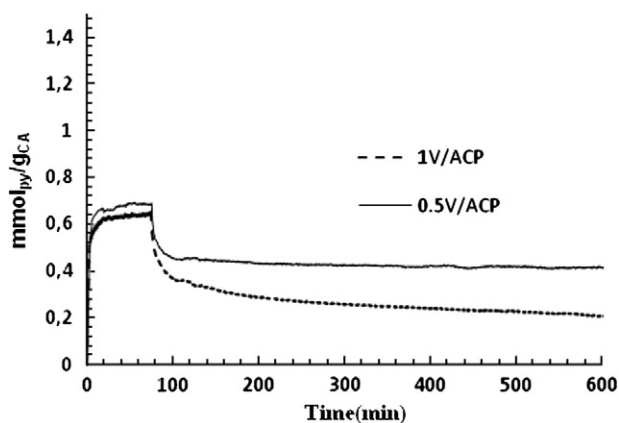


Fig. 1. Pyridine adsorption thermogravimetric experiments.

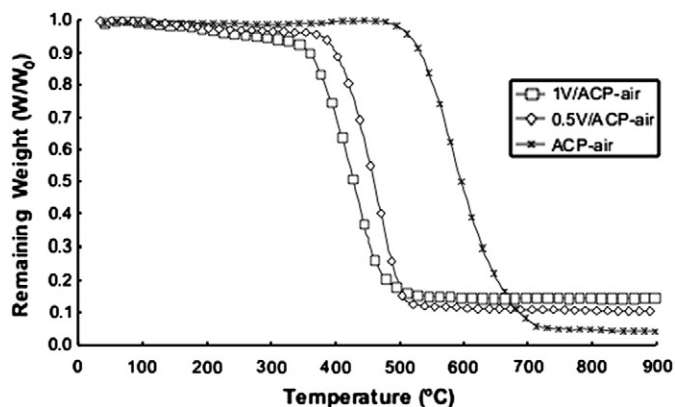


Fig. 2. Thermogravimetric analyses in air (10 min⁻¹) of ACP, 1 V/ACP and 0.5 V/ACP.

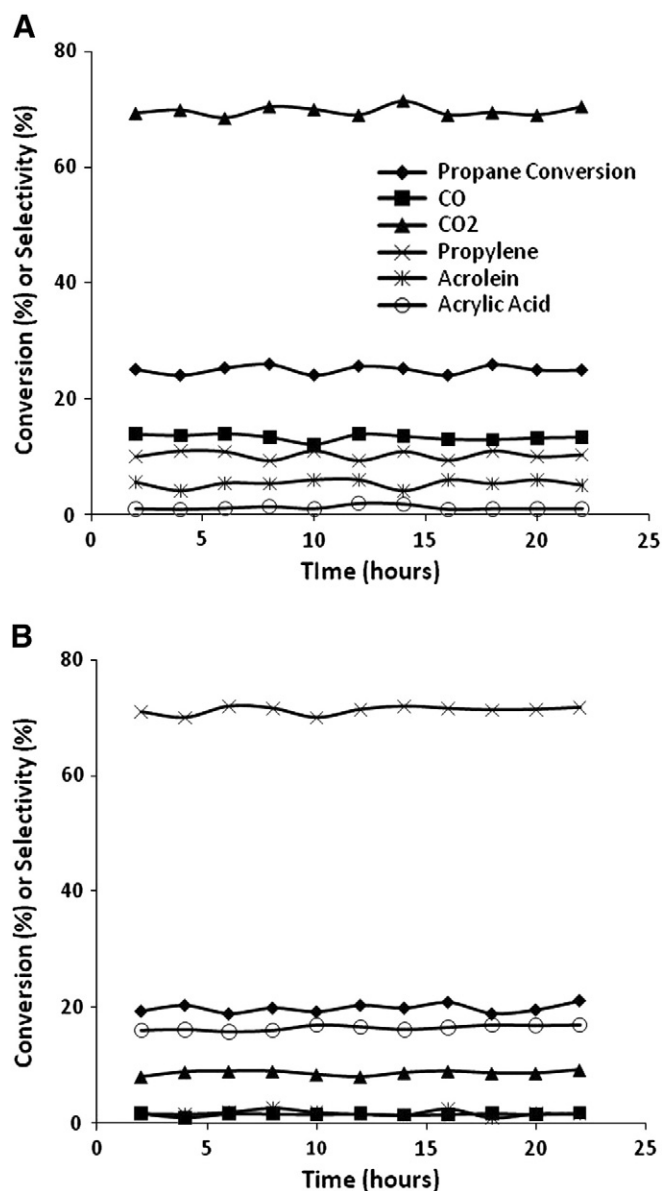


Fig. 3. Conversion and selectivity values versus time on stream for 0.5 V/ACP (A) and 1 V/ACP (B) catalysts. Reaction conditions: T = 350 °C, total flow 40 ml/min; feed composition (% volume), C₃H₈/O₂/H₂O/He (12.5/20.4/15.9/49.1), 200 mg of catalyst.

strong acid sites of the exposed carbon support are able to retain the reaction intermediates and transform them into the total oxidation products (CO₂ + CO), increasing the activity of the vanadium sites, but yielding mainly CO₂. In the case of 1 V/ACP sample, with P/V = 1.5 (Table 2), the sample has a lower amount of acid sites (Fig. 1), being the catalyst selective for the partial oxidation products.

Fig. 4 shows the in situ Raman spectra of dehydrated 1 V/ACP before and after propane oxidation reaction; Raman spectra of 0.5 V/ACP are not shown because due to the low amount of vanadium species on the carbon material, they are not detected by this technique. The two broad Raman bands, near 1370 and 1600 cm⁻¹ are typical of carbon materials and are detected before and after the catalytic tests. Two bands near 990 cm⁻¹ and 930 cm⁻¹ become apparent after being used in reaction; these new Raman bands belong to the most intense Raman modes of (VO)₂P₂O₇ and VOPO₄ phases [19], in which vanadium is present as V⁴⁺ and V⁵⁺, respectively. The coexistence of two oxidation states for vanadium ions is consistent with the XPS data. These results indicate that, during propane oxidation, VPO species form on the surface of the carbon support.

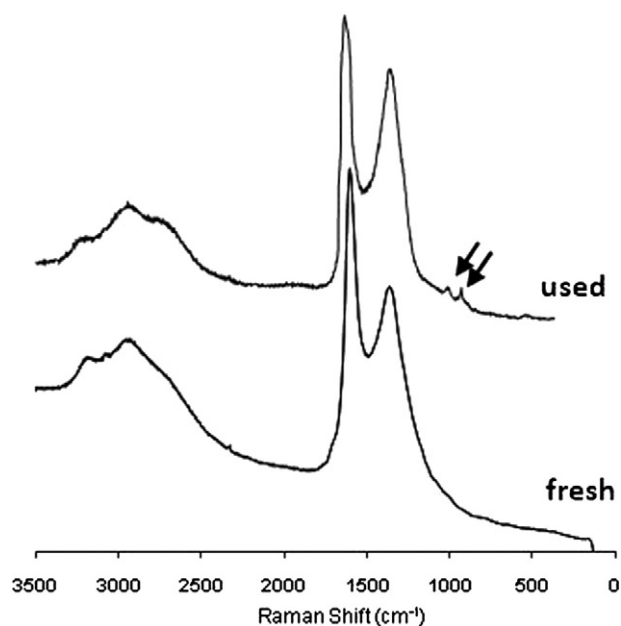


Fig. 4. Raman spectra of fresh and used 1 V/ACP catalyst.

Activation of orange skin with phosphoric acid generates an activated carbon material resistant to oxidizing conditions up to 500 °C. Such carbon material is a non-expensive material obtained by revalorization of a biomass residue. The supported VPO phases form when this activated carbon is impregnated with vanadium and reacted at the operation conditions. These catalysts show high BET surface area [21]. It is expected that the stabilization of reduced vanadium species by carbon support accounts for their high selectivity to partial oxidation products, as acrylic acid.

4. Conclusions

To the best of our knowledge, we are reporting for the first time the use of an oxidation-resistant activated carbon as catalyst support during the partial oxidation of propane. The use of such support derives to the revalorization of a biomass waste into a high valuable

catalytic material. The biomass activation process with phosphoric acid produces activated carbons with strong acid sites and highly oxidation resistance due to the presence of stable surface phosphorus groups. The subsequent impregnation with vanadium oxide species of this support can lead to the formation of surface VPO active phases, selective for the partial oxidation of propane to propylene and acrylic acid.

Acknowledgements

The Spanish Ministry of Science and Innovation funded this study under projects CTQ2009-14262 and CTQ2008/04261/PPQ. Authors thank M.J. Valero-Romero and A. Gallardo for their help with the pyridine adsorption experiments. R.L.M. thanks MAEC-AECID (Spain) for his pre-doctoral fellowship and Elizabeth Rojas García for her help with catalytic tests.

References

- [1] M.M. Lin, *Appl. Catal. A Gen.* 250 (2003) 287.
- [2] R.K. Grasselli, C.G. Lugmair, A.F. Volpe Jr., *Top. Catal.* 50 (2008) 66–73.
- [3] F. Ivars, B. Solsona, P. Botella, M.D. Soriano, J.M. López Nieto, *Catal. Today* 141 (2009) 294–299.
- [4] V.V. Gulians, R. Bhandari, J.N. Al-Saedi, V.K. Vasudevan, R.S. Soman, O. Guerrero-Pérez, M.A. Bañares, *Appl. Catal. A Gen.* 274 (2004) 123–132.
- [5] H.-G. Lintz, S.P. Müller, *Appl. Catal. A Gen.* 357 (2009) 178–183.
- [6] X.-K. Li, W.-J. Ji, J. Zhao, Z. Zhang, C.-T. Au, *Appl. Catal. A Gen.* 306 (2006) 8–16.
- [7] F. Rodríguez-Reinoso, *Carbon* 36 (1998) 159–175.
- [8] J.M. Rosas, J. Bedia, J. Rodríguez-Mirasol, T. Cordero, *Fuel* 88 (2009) 19.
- [9] J. Bedia, R. Ruiz-Rosas, J. Rodríguez-Mirasol, T. Cordero, *AIChE* 56 (2010) 1557–1568.
- [10] J. Bedia, R. Ruiz-Rosas, J. Rodríguez-Mirasol, T. Cordero, *J. Catal.* 271 (2010) 33–42.
- [11] J.M. Rosas, J. Bedia, J. Rodríguez-Mirasol, T. Cordero, *Ind. Eng. Chem. Res.* 47 (2008) 1288–1296.
- [12] B. Frank, J. Zhang, R. Blume, R. Schlögl, D.S. Su, *Angew. Chem. Int. Ed.* 48 (2009) 6913–6917.
- [13] F. Marquez-Montesinos, T. Cordero, J. Rodríguez-Mirasol, J.J. Rodríguez, *Fuel* 81 (2002) 423–429.
- [14] Y. El-Sayed, T. Bandosz, *J. Col. Inter. Sci.* 273 (2004) 64–72.
- [15] M.O. Guerrero-Pérez, L.J. Alemany, *Appl. Catal. A* 341 (2008) 119.
- [16] M.O. Guerrero-Pérez, M.A. Bañares, *J. Phys. Chem. C* 111 (2007) 1315.
- [17] J.C. Vèdrine, E.K. Novakova, E.G. Derouane, *Catal. Today* 81 (2003) 247.
- [18] M. Roussel, M. Bouchard, K. Karim, S. Al-Sayari, E. Bordes-Richard, *Appl. Catal. A* 308 (2006) 62.
- [19] Z.-Y. Xue, G.L. Schrader, *J. Phys. Chem. B* 103 (1999) 9459–9467.
- [20] J. Bedia, J.M. Rosas, D. Vera, J. Rodríguez-Mirasol, T. Cordero, *Catal. Today* 158 (2010) 89–96.
- [21] Spanish Patent Pending (P201030506), April 7th 2010.